Two New Co(II) and Ni(II) Complexes with 3-(2-Pyridyl)pyrazole-Based Ligand: Synthesis, Crystal Structures, and Bioactivities

Chun-Sen LIU,[a] Hang ZHANG,[b] Ran CHEN,[b] Xue-Song SHI,[a] Xian-He BU,*[,a] and Ming YANG*[,b]

[a] *Department of Chemistry, Nankai University; Tianjin 300071, P. R. China: and* [b] *State Key Laboratory of Natural and Biomimetic Drugs, Peking University; Beijing 100083, P. R. China.* Received December 27, 2006; accepted April 16, 2007

Two new Co(II) and Ni(II) complexes exhibiting DNA cytotoxic activities with 3-(2-pyridyl)pyrazole-based ligand, $[Co(L)_3](ClO_4)_2$ (1) and $[Ni(L)_3](ClO_4)_2$ (2) (L=1-[3-(2-pyridyl)-pyrazol-1-ylmethyl]-naphthalene) were synthesized and structurally characterized. Both 1 and 2 crystallized in the monoclinic system, space group *P*2(1)/*c*, for 1, *a*=12.8324(8), *b*=12.1205(8), *c*=33.27(2) Å, β=93.92(3)° and *Z*=4; for 2, *a*=12.8764(3), *b*=12.1015(3), *c*=33.2415(9) Å, β=93.998(1)° and *Z*=4. Among them, the Co(II) and Ni(II) ions were all coordinated by six N donors from three distinct L ligands. In addition, the cytotoxic activities of 1, 2 and L *in vitro* were evaluated against three different cancer cell lines HL-60 (human leukemia), BGC-823 (stomach cancer) and MDA-MB-435 (mammary cancer), respectively. The results showed that 1 exhibited significantly high cytotoxic activities against HL-60 and moderate activities against BGC-823 and MDA-MB-435. In order to further investigate the relationships between structures and DNA-binding behaviors of these complexes, the interactions of 1, 2 and L with calf thymus DNA (CT-DNA) were then subjected to thermal denaturation, viscosity measurements and spectrophotometric methods. The results indicated that 1 and 2 intercalated with DNA *via* L ligand. The intrinsic binding constants of 1, 2 and L with DNA were 1.6×10^4, 5.6×10^3 and 2.76×10^3 M^{-1}, respectively.

Key words Co(II) and Ni(II) complexes; crystal structure; cytotoxic activity; DNA-binding behavior; 1-[3-(2-pyridyl)pyrazole-1-ylmethyl]naphthalene

Over the past decades, investigations on DNA interactions with transition metal complexes, especially for those containing multidentate aromatic ligands, have aroused considerable interests owing to their potential applications as new therapeutic agents and interesting properties that make them as possible probes of DNA structure and conformation.[1,2] The studies on DNA metallointercalators, which can react at specific sites along a DNA strand as reactive models for protein-nucleic acid interactions, have provided us with some effective routes toward rational drug design as well as approaches to develop sensitive chemical probes for DNA.[3—9] Among them, a number of transition metal complexes with planar aromatic heterocyclic ligands have been used as the probes for DNA secondary structure and therapeutic agents. Usually, their anti-tumor activities can increase more or less compared with those of either the free ligands or metal ions alone, which may be due to the different binding properties of these complexes to DNA.[10—13]

It is necessary to understand the DNA binding properties for developing new potential DNA targeting anti-tumor drugs. In general, metal complexes interact with double helix DNA in either non-covalent or covalent way, the former including three binding modes, namely, intercalation, groove binding and external static electronic effects. In these interactions, it should be pointed out that intercalation is a significantly important binding mode to DNA. In fact, DNA intercalators are some small molecules that contain a heterocyclic functional group with the structure of planar aromatic ring, which can insert and stack between the base pairs of double-helical DNA. Meanwhile, the intercalative capability of DNA metallointercalators appears to be influenced by several factors such as the planarity of ligand, atom type of ligand donor and the coordination geometry.[14—16] Moreover, the types of different metal ions and their flexible valences, which usually are responsible for the coordination geometry of complexes, also have significant influences on the intercalating ability of transition metal complexes to DNA.[17,18]

In our previous work, a new 3-(2-pyridyl)pyrazole-based ligand **L** (see Chart 1) and its Cu(II), Zn(II) and Cd(II) complexes, namely $[Cu(\mathbf{L})_3](ClO_4)_2$, $[Cu(\mathbf{L})_2(NO_3)](NO_3)(H_2O)_{0.5}(CH_3OH)_{0.5}$, $[Zn(\mathbf{L})_3](ClO_4)_2(H_2O)_2$, $[Cd(\mathbf{L})_2(NO_3)_2](H_2O)_3$, and $[Cd(\mathbf{L})_2(ClO_4)(CH_3OH)](ClO_4)(H_2O)_{0.25}(CH_3OH)$, have been synthesized and characterized.[19,20] Obviously, the Cu(II) complexes were found to possess higher affinity to DNA and cytotoxic activity against different tested cancer cell lines (such as HL-60, BGC-823 and MDA-MB-435) as compared with Zn(II) and Cd(II) complex as well as the free ligand **L**. In attempt to further touch more insights into the relationship between structures and DNA-binding properties of such transition metal complexes, as well as to develop new useful DNA probes, herein, we report the synthesis and crystal structures of another two new complexes with **L** ligand, $[Co(\mathbf{L})_3](ClO_4)_2$ (**1**) and $[Ni(\mathbf{L})_3](ClO_4)_2$ (**2**). Moreover, the binding behaviors of these compounds with calf thymus DNA (CT-DNA) have been investigated in detail by thermal denaturation, viscosity measurements, and spectrophotometric titration.

Results and Discussion

Synthesis and General Characterization Complexes **1** and **2** were prepared by the reactions of $Co(ClO_4)_2\cdot6H_2O$ and $Ni(ClO_4)_2\cdot6H_2O$ with ligand **L** under the same conditions. The IR spectra for the two complexes showed the absorption bands resulting from the skeletal vibrations of the aromatic rings in 1600—1400 cm^{-1} region. Their IR spectra also ex-

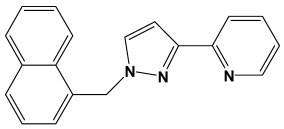

L

Chart 1

* To whom correspondence should be addressed. e-mail: buxh@nankai.edu.cn; yangm@bjmu.edu.cn

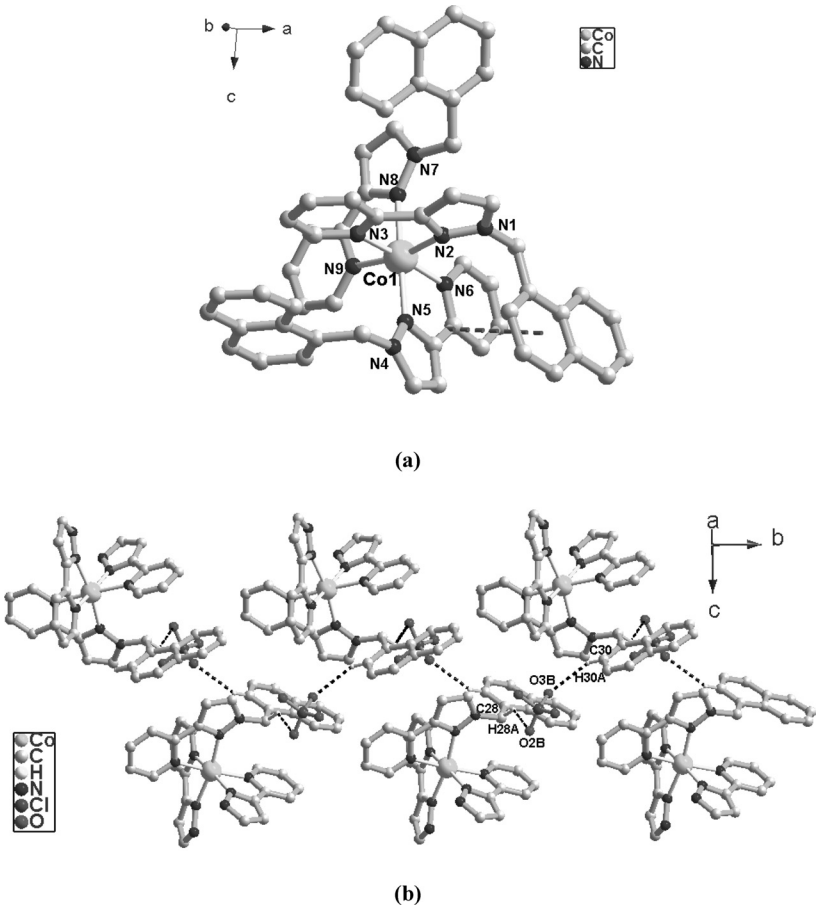

Fig. 1. View of (a) the Coordination Environment of Co(II) Ions in **1** Showing the Intramolecular π–π Stacking Interactions and (b) the 1D Chain Linked by the Intermolecular C–H···O H-Bonding Interactions (ClO_4^-, H-Atoms and Part of Naphthalene Rings Omitted for Clarity)

hibited the characteristic bands of perchlorate anions at *ca.* 622 and *ca.* 1100 cm^{-1}. It should be noted that, due to the coordination of the pyridyl rings of ligands, the strong absorption band at *ca.* 1575 cm^{-1} resulting from the skeletal vibrations of the aromatic rings shifted to *ca.* 1610 cm^{-1}. In addition, the results of elemental analyses for the two complexes were in agreement with the theoretical requirements of their compositions according to X-ray analysis results.

X-Ray Crystallography $[Co(\mathbf{L})_3](ClO_4)_2$ (**1**): The mononuclear structure of **1** consisted of discrete $[Co(\mathbf{L})_3]^{2+}$ and two ClO_4^-. The view of **1** is shown in Fig. 1 with uncoordinated ClO_4^- omitted for clarity and the selected bond lengths and angles are listed in Table 1. The coordination geometry around the Co(II) center could be described as a distorted octahedron with N(2)–N(3)–N(6)–N(9) as the basal plane, and N(5) and N(8) atoms from two distinct **L** ligands on the axial sites. The Co(II) center slightly deviates from the basal plane by *ca.* 0.0365 Å. **L** adopts *N*,*N*-bidentate chelating coordination mode to form two five-membered chelating cycles (Co–N–C–C–N) with the Co(II) center. All the bond angles around Co(II) ranged from 76.23° to 77.10°. Furthermore, the bond distances of Co(1)–N(5) [2.155(5) Å and Co(1)–N(8) [2.213(4) Å] were a little longer than those of the other Co–N bonds (distances from 2.122(4) to 2.136(4) Å) and all the Co–N bond distances and angles around each Co(II) center fall into the normal ranges for such coordination complexes (see Table 1).[22,23]

Table 1. Selected Bond Lengths and Angles (Å, °) for Complex **1**

Co(1)–N(9)	2.122(4)	Co(1)–N(6)	2.130(5)
Co(1)–N(2)	2.131(4)	Co(1)–N(3)	2.136(4)
Co(1)–N(5)	2.155(5)	Co(1)–N(8)	2.213(4)
N(9)–Co(1)–N(6)	86.41(17)	N(9)–Co(1)–N(2)	168.26(16)
N(6)–Co(1)–N(2)	102.14(16)	N(9)–Co(1)–N(3)	95.31(17)
N(6)–Co(1)–N(3)	175.41(18)	N(2)–Co(1)–N(3)	76.78(17)
N(9)–Co(1)–N(5)	97.80(17)	N(6)–Co(1)–N(5)	77.1(2)
N(2)–Co(1)–N(5)	92.01(16)	N(3)–Co(1)–N(5)	98.44(18)
N(9)–Co(1)–N(8)	76.23(17)	N(6)–Co(1)–N(8)	94.82(18)
N(2)–Co(1)–N(8)	94.85(15)	N(3)–Co(1)–N(8)	89.72(14)
N(5)–Co(1)–N(8)	170.36(17)		

In addition, due to the flexibility of the methylene group, the naphthalene group of **L** could turn freely to offer a suitable space for intramolecular π–π stacking interactions with the pyridyl-pyrazole ring from other **L** with the centroid–centroid distances of 3.703 Å, average interplanar separation of 3.553 Å and dihedral angle of 7.4°, which further stabilize the structure of complex **1**.[24] Furthermore, the adjacent $[Co(\mathbf{L})_3]^{2+}$ units are linked together into 1D chains *via* the intermolecular C–H···O H-bonding interactions between the O-atoms from uncoordinated ClO_4^- anions and H-atoms from methylene groups and naphthalene rings of **L** [C(28)–H(28A)···O(2B) and C(30)–H(30A)···O(3B), symmetry code B = $-x+3/2$, $y+1/2$, $-z+1/2$] (Fig. 1b).[25] The separations of C(28)···O(2B) and C(30)···O(3B) are 3.1542

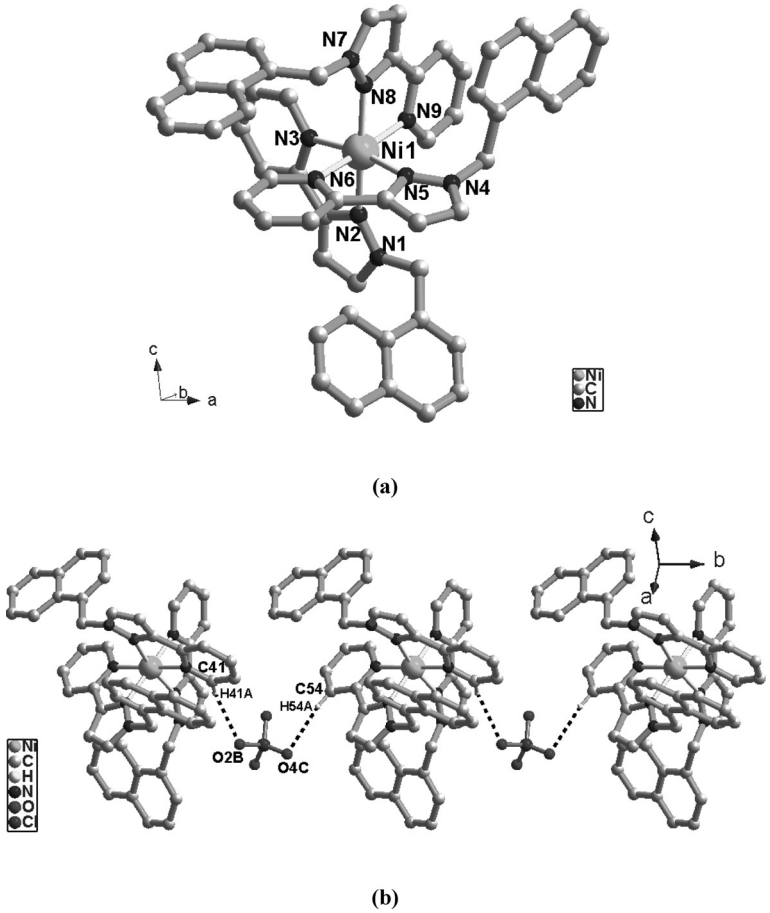

Fig. 2. View of (a) the Coordination Environment of Ni(II) Ions in **2** and (b) the 1D Chain Linked by the Intermolecular C–H···O H-Bonding Interactions (ClO_4^- and H-Atoms Omitted for Clarity)

and 3.4156 Å, with the angles of C(28)–H(28A)···O(2B) and C(30)–H(30A)···O(3B) of 123 and 147°, respectively, which further enhance the stabilities of **1** in the solid state.

$[Ni(\mathbf{L})_3](ClO_4)_2$ (**2**): Similar to **1**, the structure of **2** also consists of mononuclear $[Ni(\mathbf{L})_3]^{2+}$ and two uncoordinated ClO_4^-. As shown in Fig. 2, the coordination geometry around each Ni(II) also could be described as a distorted octahedron with N(3)–N(5)–N(6)–N(9) as the basal plane, N(2) and N(8) atoms from two distinct **L** on the axial sites. The Ni(II) center deviates from the basal plane by *ca.* 0.0279 Å. All the Ni–N bond distances [from 2.097(6) to 2.169(3) Å] and the bond angles around each Ni(II) center [from 77.66(13)° to 176.09(14)°] were in the normal range expected for such coordination complexes (see Table 2).[22,23] In addition, **L** also adopts *N*,*N*-bidentate chelating coordination mode to form two five-membered chelating cycles (Ni–N–C–C–N) with Ni(II) center.

Different from **1**, in **2**, the centroid–centroid separations of the naphthalene rings with pyridyl-pyrazole rings from adjacent **L** were in the range of 3.887—4.128 Å, showing no obvious existence of intramolecular weak π–π stacking interactions.[24] However, similar to **1**, there are obvious intermolecular C–H···O H-bonding interaction between the O-atoms from the uncoordinated ClO_4^- anions and H-atoms of pyridyl rings of ligands **L** (C(41)–H(41A)···O(2B) and C(54)–H(54A)···O(4C)) [symmetry code B=$-x+1$, $-y+2$, $-z$ and C=$-x+1$, $-y+1$, $-z$] with the separations of 3.2151 and 3.4715 Å for C(41)···O(2B) and C(54)···O(4C) and the angles of 126 and 159° for C(41)–H(41A)···O(2B) and C(54)–H(54A)···O(4C), respectively (see Fig. 2b).[25]

Table 2. Selected Bond Lengths and Angles (Å, °) for Complex **2**

Ni(1)–N(9)	2.096(3)	Ni(1)–N(3)	2.097(3)
Ni(1)–N(5)	2.102(3)	Ni(1)–N(6)	2.104(3)
Ni(1)–N(8)	2.121(4)	Ni(1)–N(2)	2.169(3)
N(9)–Ni(1)–N(3)	87.53(13)	N(9)–Ni(1)–N(5)	100.66(13)
N(3)–Ni(1)–N(5)	169.57(12)	N(9)–Ni(1)–N(6)	176.09(14)
N(3)–Ni(1)–N(6)	94.13(12)	N(5)–Ni(1)–N(6)	78.11(12)
N(9)–Ni(1)–N(8)	78.82(16)	N(3)–Ni(1)–N(8)	96.54(14)
N(5)–Ni(1)–N(8)	91.42(12)	N(6)–Ni(1)–N(8)	97.46(14)
N(9)–Ni(1)–N(2)	93.64(14)	N(3)–Ni(1)–N(2)	77.66(13)
N(5)–Ni(1)–N(2)	95.24(11)	N(6)–Ni(1)–N(2)	90.17(12)
N(8)–Ni(1)–N(2)	170.78(13)		

Cytotoxicity Studies The *in vitro* cytotoxicity of complexes **1** and **2**, and ligand **L** was examined in three human cancer cells lines, HL-60 human leukemia, BGC-823 human stomach and MDA-MB-435 human mammary. The results of the testing are summarized in Table 3. The ligand **L** showed no cytotoxicity activity against these three cell lines, whereas **1** and **2** showed obviously cytotoxic activities, furthermore following the order **1**>**2**. This directly indicated that the cytotoxicity of ligand increased after the formation of metal complexes, which may be attributed to the extended planar structure induced by the p–π* conjugation from the chelation of

Table 3. Inhibitory Rates of **1**, **2** and **L** against Different Cancer Cell Lines ([Compound]=1.0×10^{-5} M)

Compounds	HL-60	BGC-823	MDA-MB-435
L	$-5^{a)}$	7	3
1	89	40	48
2	1	12	12

a) The negative value of inhibitory rate, calculated directly from the test, means that the compound caused proliferation of the cancer cells.

metal ions with the ligand **L**. Moreover, when the results were compared with that of Cu(II) and Zn(II) complexes previously reported,[19—21] it can be seen that **1** showed equivalently cytotoxicity against HL-60 but lower activity against BGC-823 and MDA-MB-435. On the other hand, among these three cancer cells lines, HL-60 was the most sensitive to the tested compounds (**1**, **2** and **L**) with inhibitory rate ranged from −5.42 to 89.29%. These results of biological tests *in vitro* will prompt us to further explore more studies on the binding mode of these complexes to DNA.

Determination of Binding Mode to DNA Thermal denaturation, intrinsic binding constant determination and viscosity measurements were conducted to explore the binding mode of the tested compounds (**1**, **2** and **L**) to DNA.

Thermal Denaturation: DNA melting was observed when double-stranded DNA molecules were heated and separated into two single strands, which was due to disruption in intermolecular forces between DNA base pairs. Changes in the thermodynamic stability of double-stranded DNA are thought to play an important role in the recognition and processing of DNA modified with covalent and noncovalent drug adducts.[26] The melting curves of CT-DNA in the presence and absence of **1**, **2** and **L** are shown in Fig. 3. The melting point of free CT-DNA was 61.0 °C under our experimental conditions. **1**, **2** and **L** increased the T_m value of DNA by 2.8 °C, 1.4 °C and 0.3 °C, respectively, which indicated that these compounds had a capability to stabilize the DNA duplex. Therefore, it can be supposed that the binding of these compounds to DNA might involve an intercalative behavior.[27] Moreover, the ΔT_m values of **1** and **2** were higher than that of free ligand **L**, probably owing to the extension of π-system of the free ligand alone and stacking effect on DNA duplex stabilization. At the same time, this was also reflected in the following viscosity and binding constants measurements.

Viscosity Measurements: Hydrodynamic measurement that is sensitive to length change is, in the absence of crystallographic data, regarded as the most critical tests of a binding mode in solution.[28] Classical intercalative agents can separate the base pairs to accommodate the binding ligands, then causing elongation of the DNA double helix and increasing its viscosity. However, a partial or nonclassical intercalation of ligand may bend the DNA helix, resulting in the decrease of its effective length and, concomitantly, its viscosity.[29] In addition, some other transition metal complexes, which bind through non-intercalative mode such as groove-face and electrostatic interactions, typically cause less pronounced or no change in the DNA solution viscosity.[30] The changes in the specific relative viscosities upon the addition of the compounds to DNA solution were examined. As shown in Fig. 4, the viscosities of DNA increased with the increment of [compound]/[DNA] ratio, and changes in the viscosities caused by **1** and **2** were similar to those by classical intercalators[2] but sharper than free ligand **L**. Those results indicated that **1** and **2** bound to DNA by an intercalative mode and **1** more tightly than **2** did, which also agreed well with the results of thermal denaturation experiment.

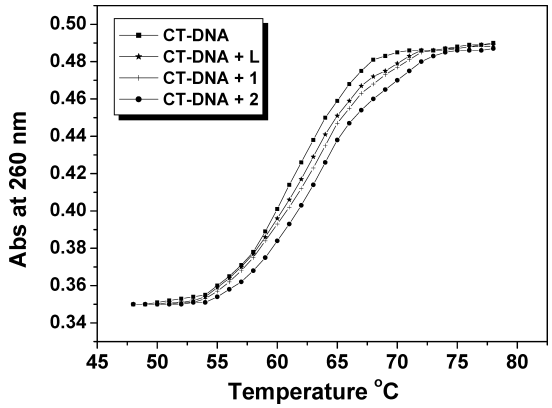

Fig. 3. Melting Curves of CT-DNA in the Absence and Presence of Compounds **1**, **2** and **L**

[DNA]=5.0×10^{-5} M and [compound]=2.0×10^{-5} M.

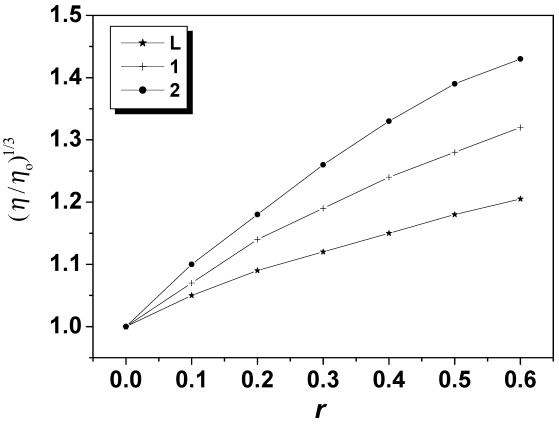

Fig. 4. Effects of Increasing Amounts of the Compounds **1**, **2** and **L** on the Relative Viscosities of CT-DNA at 30.0 (±0.1) °C

[DNA]=7.2×10^{-5} M and r=[compound]/[DNA].

Determination of Binding Constants: To investigate quantitatively the binding affinities of these compounds binding to DNA, the binding constants K_b of **1**, **2** and **L** were determined by spectrophotometric titration method, according to the site exclusion equation of McGhee and Von Hippel:

$$\nu/c=K_b(1-n\nu)\{(1-n\nu)/[1-(n-1)\nu]\}^{(n-1)}$$

where ν is the ratio of the bound compound to DNA base pairs, c is the free compound concentration, K_b is the intrinsic binding constant and n is the binding site size. K_b and n were determined by Scatchard plot analyses using a non-linear least-square procedure (Program Knwfit). The binding constants obtained for **1**, **2** and **L** were 1.6×10^4, 5.6×10^3 and 2.76×10^3 M^{-1}, respectively, and their corresponding n values (namely the numbers of binding sites) were 1.8, 1.8 and 1.64. These results revealed that the affinities of these complexes binding to DNA showed significant increase upon the chelation between the free ligand **L** and metal center, which further resulted in the extension of π-system of ligand,

leading to the ligand stacking more strongly with the DNA duplex. The obvious existence of intramolecular face-to-face π–π stacking interactions may be responsible for the higher K_b value of these complexes, especially for **1**.

Conclusion

Two new Co(II) (**1**) and Ni(II) (**2**) complexes with the 3-(2-pyridyl)pyrazole-based ligand **L** (**L**=1-[3-(2-pyridyl)-pyrazol-1-ylmethyl]-naphthalene) have been synthesized and characterized. Their crystal structures were determined by X-ray diffraction analysis. According to our experimental results in this study as well as the previous work,[19] complexes **1** and **2** were not dissociated under PE buffer system of biological conditions. DNA binding behaviors of **1**, **2** and **L** with CT-DNA were investigated *via* thermal denaturation, viscosity measurements and spectrophotometric titration method. The results of viscosity measurements indicated that **1** and **2** bound to DNA in an intercalative mode through their ligand **L**. The affinity of these compounds binding to DNA follows the order **1**>**2**>**L**, which is in good agreement with the results of T_m values according to thermal denaturation measurement. The biological assays *in vitro* further showed that **1** possessed high cytotoxic activities against HL-60 and moderate against BGC-823 and MDA-MB-435 cell lines. Further work is in progress to elucidate the detailed mechanisms of anti-tumor activity of these compounds in our lab.

Experimental

Materials and Measurements All the reagents for syntheses were commercially available and used as received or purified by standard method prior to use. 3-(2-Pyridyl)-pyrazole[31,32] and **L**[19—21,35,36] were synthesized according to the reported procedures. Elemental analyses were performed on a Perkin-Elemer 240C analyzer and IR spectra on a Tensor 27 OPUS (Bruker) FT-IR spectrometer with KBr pellets. ^{1}H-NMR spectra were recorded on a Bruker AC-P500 spectrometer (300 MHz) at 25 °C in $CDCl_3$ with tetramethylsilane as the internal reference.

Calf thymus DNA (CT-DNA) was dissolved in PE buffer (1 mM NaH_2PO_4, 0.1 mM EDTA and pH=7.0). The UV absorbance ratio $\lambda_{260}/\lambda_{280}$ was 1.8—1.9, indicating that the DNA was sufficiently free of protein.[33] The CT-DNA concentration per nucleotide was determined by absorption spectroscopy using the molar absorption coefficient of 6600 $mol^{-1}\,cm^{-1}$ at 260 nm.[34] Also, doubly distilled water was used to prepare PE buffer.

Preparation of Complexes $[Co(L)_3](ClO_4)_2$ (1) The reaction of **L** (0.3 mmol) with $Co(ClO_4)_2\cdot 6H_2O$ (0.1 mmol) in MeOH (10 ml) for a few minutes afforded orange solid, which was filtered. Then, to this mixed system 5 ml of acetonitrile was added and stirred for about 30 min until the solid was dissolved. The resultant solution was kept at room temperature and yellow single crystals suitable for X-ray analysis were obtained by slow evaporation of the solvent after several days. Yield: *ca.* 40%. IR (KBr pellet, cm^{-1}): 3069w, 1610s, 1569m, 1507m, 1439s, 1366s, 1328m, 1287w, 1245s, 1195w, 1163s, 1097vs, 958s, 904s, 797s, 771m, 623s 529w. *Anal.* Calcd for $C_{57}H_{45}Cl_2CoN_9O_8$: C, 61.46; H, 4.07; N, 11.32. Found: C, 61.71; H, 3.90; N, 11.19%.

$[Ni(L)_3](ClO_4)_2$ (**2**): **2** was prepared and characterized by the similar procedures as that for **1** as purple block. Yield: *ca.* 50%. IR (KBr pellet, cm^{-1}): 3071w, 2016w, 1611s, 1570m, 1533s, 1507s, 1442vs, 1369s, 1328w, 1287w, 1246m, 1163br, 1094vs, 863w, 777vs, 692w, 622vs, 528w, 422w. *Anal.* Calcd for $C_{57}H_{45}Cl_2NiN_9O_8$: C, 61.48; H, 4.07; N, 11.32. Found: C, 61.21; H, 4.18; N, 11.13%.

CAUTION: Although we met no problems in handling perchlorate salts and their complexes during this work, these should be treated with great caution owing to their potential explosive nature.

X-Ray Structure Determination Single-crystal X-ray diffraction measurement for complexes **1**—**2** were carried out on a Bruker Smart 1000 CCD diffractometer equipped with a graphite crystal monochromator situated in the incident beam for data collection at 293(2) K. The determinations of unit cell parameters and data collections were performed with Mo$K\alpha$ radiation (λ=0.71073 Å) and unit cell dimensions were obtained with least-square refinements. The program SAINT[37] was used for integration of the diffraction profiles. The structure was solved by direct methods using the SHELXS program of the SHELXTL package and refined with SHELXL[38] All non-hydrogen atoms were located in successive difference Fourier syntheses. The final refinement was performed by full matrix least-square methods with anisotropic thermal parameters for non-hydrogen atoms on F^2. The hydrogen atoms were added theoretically, riding on the concerned atoms and refined with fixed thermal factors. Crystallographic data and experimental details for structural analyses are summarized in Table 4. The crystal data files in cif format are listed in the supplemental material.

Table 4. Crystal Data and Structure Refinement Summary for Complexes **1**—**2**

	1	**2**
Empirical formula	$C_{57}H_{45}Cl_2CoN_9O_8$	$C_{57}H_{45}Cl_2NiN_9O_8$
Formula weight	1113.85	1113.63
Crystal system	Monoclinic	Monoclinic
Space group	*P*2(1)/*c*	*P*2(1)/*c*
Unit cell dimensions (Å, °)		
a	12.8324(8)	12.8764(3)
b	12.1205(8)	12.1015(3)
c	33.27(2)	33.2415(9)
β	93.92(3)	93.998(1)
Volume (Å^3)	5162.5(6)	5167.2(2)
Z	4	4
D_{calcd} (g/cm^3)	1.433	1.432
μ (mm^{-1})	0.503	0.545
F(000)	2300	2304
Range of *h*, *k*, *l*	−13/15, −14/11, −40/40	−15/15, −14/14, −40/40
Reflections collected/unique	42771/9612	45935/9591
Max. and min. transmission	0.9284, 0.8721	0.9227, 0.8757
Data/restraints/parameters	9612/0/695	9591/0/694
Goodness-of-fit on F^2	0.917	0.980
$R^{a)}$ and $wR^{b)}$ [$I>2\sigma(I)$]	0.0718, 0.1751	0.0627, 0.1696
Largest diff. peak & hole (e/Å^3)	0.743, −0.366	0.950, −0.445

a) $R=\Sigma(||F_o|-|F_c||)/\Sigma|F_o|$; *b*) $wR=[\Sigma w(|F_o|^2-|F_c|^2)^2/\Sigma w(F_o^2)]^{1/2}$.

Cytotoxicity Assay Cytotoxic activities of **1** and **2** and ligand **L** were conducted by the tetrazolium salt MTT (MTT=3-(4,5-dimethylthiazol-2-yl)-2,5-diphenyl-tetrazolium bromide) reduction assay.[39] The following human cancer cell lines were used: HL-60 human leukemia, BGC-823 human stomach and MDA-MB-435 human mammary. Having grown in RPMI 1640 medium supplemented with 10% freshly inactivated fetal calf serum (FCS) and antibiotics, the cells harvested from exponential phase (2×10^5 per ml) were seeded equivalently into a 96-well plate, the tested compounds were added at a concentration maintained at 10 μmol l^{-1}. The plate was maintained at 37 °C in a humidified atmosphere of 5% CO_2 incubated for 48 h, MTT solution at an appropriate concentration (1 mg ml^{-1}) was then added to each well. After incubation at 37 °C for 4 h, 100 μl of 0.04 mol l^{-1} HCl in isopropanol was added to each well and mixed thoroughly to dissolve the dark blue crystals. The measurement of absorbance of the solution related to the number of live cells was performed on a Bio-Rad Model 450 Microplate reader at 570 nm and the inhibitory rate was calculated.[40]

DNA-Binding Experiments Thermal denaturation processes were followed on a WFZ-800-D_2 spectrophotometer equipped with a thermoelectric cell temperature controller (±0.5 °C) and a stirrer unit. Before the T_m measurement, a mixture solution of the title compounds and the duplexes was equilibrated for 15 min and then the temperature was increased at the rate of 0.4 °C/min. A 1-cm quartz cuvette was used. The absorbance at 260 nm was monitored for DNA in the absence and presence of the compounds. The T_m value was determined graphically for each sample from the spectral data. The ΔT_m value for each compound was calculated as the temperature difference between the compound's T_m and the free DNA's T_m.

Viscosity measurement was carried out on an Ubbelodhe viscometer, immersed in a thermostatted water bath maintained at 30±0.1 °C. The concentration of DNA was kept constant (72 μM) and that of tested compounds varied from 7.2 to 43.2 μM. The flow time was measured with a stop-watch operated manually, and each sample was measured five times and an average flow time was calculated. Data are presented as $(\eta/\eta_o)^{1/3}$ *versus* [compound]/[DNA], where η is the viscosity of DNA in the presence of tested

compounds and η_o is the viscosity of DNA alone. Viscosity values were calculated from the observed flow time of DNA-containing solutions corrected for the flow time of buffer alone (t_0), $\eta = t - t_0$.[41]

The binding constant for the interaction of DNA with compounds was obtained from absorption titration data. A fixed concentration of DNA was titrated with increasing amounts of the compound and the molar ratio of the compound to DNA ranged from 0.02 to 0.25. The absorbance rates at 300 nm were recorded after each adding using on a WFZ-800-D2 spectrophotometer and analyzed by the Program Knwift, Applied to the McGhee and Von Hippel equation.[42]

Supplementary Material Crystallographic data for the crystal structure reported in this paper have been deposited with the Cambridge Crystallographic Data Center. The CCDC deposition numbers are 271745 for $[Co(\mathbf{L})_3](ClO_4)_2$ (**1**) and 271746 for $[Co(\mathbf{L})_3](ClO_4)_2$ (**2**). This material can be obtained free of charge *via* www.ccdc.cam.ac.uk/conts/retrieving.html (or from the CCDC, 12 Union Road, Cambridge CB2 1EZ, U.K.; fax: +44 1223 336033; e-mail: deposit@ccdc.cam.ac.uk).

Acknowledgements This work was supported by the Project 863 of the Ministry of Science and Technology of China (No. 2006AA020502) and the National Natural Science Foundation of China (Nos. 20531040 and 30670415). We also thank Mr. Su-Long Xiao for technical assistances.

References

1) Erkkila K. E., Odom D. T., Barton J. K., *Chem. Rev.*, **99**, 2777—2796 (1999).
2) Haq I., Lincoln P., Suh D., Norden B., Chowdhry B. Z., Charies J. B., *J. Am. Chem. Soc.*, **117**, 4788—4796 (1995).
3) Arturo S., Giampaolo B., Giuseppe R., Maria L. G., Salvatore T., *J. Inorg. Biochem.*, **98**, 589—594 (2004).
4) Metcalfe C., Thomas J. A., *Chem. Soc. Rev.*, **32**, 215—224 (2003).
5) Navarro M., Cisneros F. E. J., Sierralta A., Fernadez M. M., Silva P., Arrieche D., Marchan E., *J. Biol. Inorg. Chem.*, **8**, 401—408 (2003).
6) Catherine H., Marguerite P., Michael R., Heinz G., Stéphanie S., Bernard M., *J. Biol. Inorg. Chem.*, **6**, 14—22 (2001).
7) Liang F., Wang P., Zhou X., Li T., Li Z. Y., Lin H. K., Gao D. Z., Zheng C. Y., Wu C. T., *Bioorg. Med. Chem. Lett.*, **14**, 1901—1904 (2004).
8) Dhar S., Chakravarty A. R., *Inorg. Chem.*, **42**, 2483—2485 (2003).
9) Krugh T. R., *Curr. Opin. Struc. Biol.*, **4**, 351—364 (1994).
10) Lewandowski W., Kalinowska M., Lewandowska H., *J. Inorg. Biochem.*, **99**, 1407—1423 (2005).
11) Monica B., Marisa B. F., Franco B., Silvia C., Giorgio P., Pieralberto T., *J. Inorg. Biochem.*, **99**, 1504—1513 (2005).
12) West D. X., Liberta A. E., Padhye S. B., Chikate R. C., Sonawane P. B., Kumbhar A. S., Yerande R. G., *Coord. Chem. Rev.*, **123**, 49—71 (1993).
13) Xu H., Zheng K. C., Deng H., Lin L. J., Zhang Q. L., Ji L. N., *New. J. Chem.*, **27**, 1255—1263 (2003).
14) Xu H., Zheng K. C., Deng H., Lin L. J., Zhang Q. L., Ji L. N., *J. Chem. Soc.*, *Dalton Trans.*, **2003**, 2260—2268 (2003).
15) Kumar C. V., Barton J. K., Turro N. J., *J. Am. Chem. Soc.*, **107**, 5518—5523 (1985).
16) Mahadevan S., Palaniandavar M., *Inorg. Chim. Acta*, **254**, 291—302 (1997).
17) Chaires J. B., *Biopolymers*, **44**, 201—215 (1997).
18) Mozaffar A., Elham S., Bijan R., Leila H., *New J. Chem.*, **28**, 1227—1234 (2004).
19) Zhang H., Liu C. S., Bu X. H., Yang M., *J. Inorg. Biochem.*, **99**, 1119—1125 (2005).
20) Chen R., Liu C. S., Zhang H., Guo Y., Yang M., Bu X. H., *J. Inorg. Biochem.*, **101**, 412—421 (2007).
21) Liu C. S., Li J. R., Zou R. Q., Zhou J. N., Shi X. S., Wang J. J., Bu X. H., *J. Mol. Struct.*, in press (2007).
22) O'Keeffe M., Brese N. E., *J. Am. Chem. Soc.*, **113**, 3226—3229 (1991).
23) Orpen A. G., Brammer L., Aleen F. H., Kennard O., Watson D. G., Taylor R., *J. Chem. Soc.*, *Dalton Trans.*, **1989**, S1—S83 (1989).
24) Janiak C., *J. Chem. Soc.*, *Dalton Trans.*, **2000**, 3885—3896 (2000).
25) Desiraju G. R., Steiner T., "The Weak Hydrogen Bond in Structural Chemistry and Biology," Oxford University Press, Oxford, 1999.
26) Baruah H., Bierbach U., *J. Biol. Inorg. Chem.*, **9**, 335—344 (2004).
27) Baruah H., Rector C. L., Monnier S. M., Bierbach U., *Biochem. Pharmacol.*, **64**, 191—200 (2002).
28) Vaidyanathan V. G., Nair B. U., *Eur. J. Inorg. Chem.*, **2003**, 3633—3638 (2003).
29) Xiong Y., He X. F., Zou X. H., Wu J. Z., Chen X. M., Ji L. N., Li R. H., Zhou J. Y., Yu K. B., *J. Chem. Soc.*, *Dalton Trans.*, **1999**, 19—24 (1999).
30) Kelly T. M., Tossi A. B., McConnell D. J., Strekas T. C., *Nucleic Acids Res.*, **13**, 6017—6034 (1985).
31) Amoroso A. J., Cargill Thompson A. M., JeVery J. C., Jones P., McCleverty J. A., Ward M. D., *J. Chem. Soc., Chem. Commun.*, **1994**, 2751—2752 (1994).
32) Brunner H., Scheck T., *Chem. Ber.*, **125**, 701—709 (1992).
33) Marmur J., *J. Mol. Biol.*, **3**, 208—218 (1961).
34) Reichmann M. F., Rice S. A., Thomas C. A., Doty P., *J. Am. Chem. Soc.*, **76**, 3047—3053 (1954).
35) Ward M. D., McCleverty J. A., Jeffery J. C., *Coord. Chem. Rev.*, **222**, 251—272 (2001).
36) Bell Z. R., Jeffery J. C., McCleverty J. C., Ward M. D., *Angew. Chem. Int. Ed.*, **41**, 2515—2518 (2002).
37) Bruker AXS SAINT Software Reference Manual, Madison, WI (1998).
38) Sheldrick G. M., SHELXTL-NT Version 5.1., Program for Solution and Refinement of Crystal Structures, University of Göttingen, Germany, 1997.
39) Freshney R. I., "Culture of Animal Cells: a Manual of Basic Technique," Wiley-Liss, New York, 1994.
40) Mosmann T., *J. Immunol. Meth.*, **65**, 55—63 (1983).
41) Zou X. H., Ye B. H., Liu J. G., Xiong Y., Ji L. N., *J. Chem. Soc.*, *Dalton Trans.*, **1999**, 1423—1428 (1999).
42) Xu Z. D., Liu H., Wang M., Xiao S. L., Yang M., Bu X. H., *J. Inorg. Biochem.*, **92**, 149—155 (2002).